International Journal of Thermophysics, Vol. 21, No. 2, 2000

Measurement of the Thermal Diffusivity of Metallic Foils and Films by the Photoacoustic Method[1]

A. Yoshida,[2,3] Y. Omae,[2] T. Kurita,[2] and S. Washio[2]

The thermal diffusivities of four kinds of metallic foils from 20 to 200 μm in thickness were measured by a photoacoustic method on the basis of the Rosencwaig and Gersho theory. The measured data for continuous foils of uniform microscopic structure almost agreed with the literature values. Measurements were also carried out on two kinds of metallic thin films with of 10 μm thickness produced by sputtering. The difference in thermal diffusivity between the foils and the sputtered films depended on the uniformity of the microscopic structure.

KEY WORDS: metal; microscopic structure; phase lag; photoacoustic effect; thermal diffusivity; thin layer.

1. INTRODUCTION

The importance of the thermophysical properties of thin films has been recognized in connection with recent progress in high-technology fields such as LSI manufacturing processes. However, the thermophysical properties of thin films produced by microscopic processes, such as PVD or CVD, may be significantly different from those of the material in bulk form.

Conventional measurement techniques such as laser flash methods cannot be applied to thin films on a substrate because the thermophysical properties of the substrate are often unknown and it is difficult to place the sensors directly on the films. In order to measure the thermophysical properties of thin films, a noncontact photoacoustic method has attracted

[1] Paper presented at the Fifth Asian Thermophysical Properties Conference, August 30–September 2, 1998, Seoul, Korea.

[2] Department of Mechanical Engineering, Okayama University, 3-1-1 Tsushima-naka, Okayama 700-8530, Japan.

[3] To whom correspondence should be addressed.

0195-928X/00/0300-0513$18.00/0

special interest. A theoretical treatment was given by Rosencwaig and Gersho [1], and a measurement technique based on the theory was used to measure the thermal diffusivity of metallic foils by Akaboroi et al. [2].

In the present study, the photoacoustic method [1] is applied to measure the thermal diffusivities of metallic thin films which are opaque and nonscattering for radiation, over a wide frequency region. The difference in thermal diffusivity between the foils and the films is discussed in connection with their fine structure.

2. PRINCIPLE OF MEASUREMENT

A sample mounted on a backing in a closed cell is irradiated by a modulated light as shown in Fig. 1. The radiation energy is periodically absorbed within the sample and translated into heat. It is transported to a thin boundary layer of gas. The heat conduction is assumed to be one-dimensional with respect to the ac component [3]. Then the expansion and the contraction of gas are repeated in the boundary layer. The resulting behavior induces a periodic variation of pressure, which is detected as sound. Information on the thermophysical properties of the sample is included in the variation of the detected sound.

The theoretical treatment is based on a theory of Rosencwaig and Gersho (RG) [1] according to which the phase lag of the photoacoustic signal for the incident modulated light φ is expressed as a function of four parameters:

$$\varphi = F[f : \beta l, l/\sqrt{\alpha}, b, g] \tag{1}$$

where f, β, l, and α are the modulation frequency of the incident radiation, the absorption coefficient of the sample, the thickness of the sample, and the thermal diffusivity of the sample, respectively. b and g indicate the ratios of the thermal effusivity of backing to sample and that of air to sample, respectively. The thermal effusivity e is defined by $e = k/\sqrt{\alpha}$, where

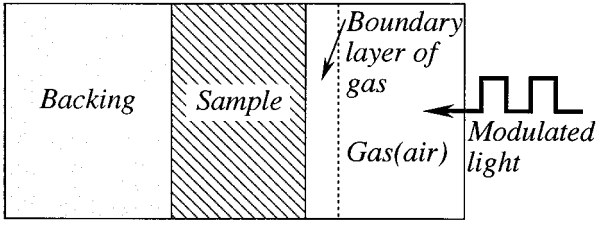

Fig. 1. One-dimensional model of a photoacoustic cell.

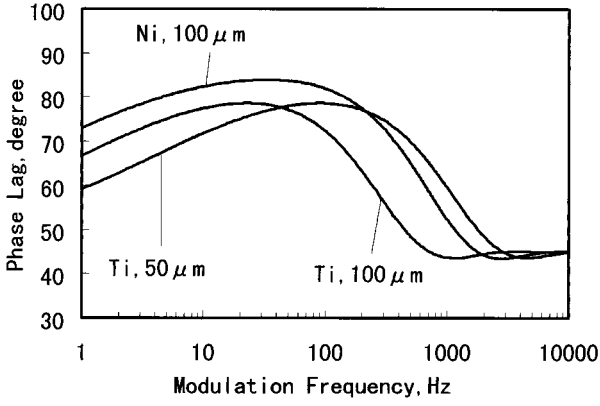

Fig. 2. Calculated results of phase lag vs. modulation frequency based on the RG theory [1].

k is the thermal conductivity. We assume that $g = 0$ because the effusivity of air is much smaller than that of the metallic sample. In the present study, the optical thickness βl is greater than 1000. As the sample is supposed to be optically thick, the phase lag is independent of the optical thickness. If we know the thickness of the sample, there are two unknown values, α and b, to be determined. These values are determined through curve fitting of the phase lag data by using a nonlinear least-squares method [4]. Even if the thermophysical properties of the backing are unknown, the thermal diffusivity of sample α can be obtained. If they are known, the thermal conductivity of the sample k is also obtained from the value b.

In order to investigate the effects of the thickness and the thermophysical properties of the sample upon the phase lag, a numerical calculation is performed based on the RG theory. Figure 2 shows the calculated results of the phase lag as a function of the modulation frequency. The values of the thermophysical properties for titanium or nickel [5] are used in the calculation. The absorption coefficient is assumed to be 10^8 m^{-1}. The backing is considered to be acrylic resins. The results indicate that the thickness affects the change of the peak frequency where the phase lag has a maximum point. The thermophysical properties affect the height of the maximum point of the phase lag and the peak frequency. In order to determine the thermal diffusivity of the sample, it is important that the measured modulation frequency includes the peak.

3. EXPERIMENTAL APPARATUS AND PROCEDURE

Figure 3 shows a diagram of the experimental apparatus. An Ar^+ laser having a wavelength of 514.5 nm with an output power of 1.5 W is

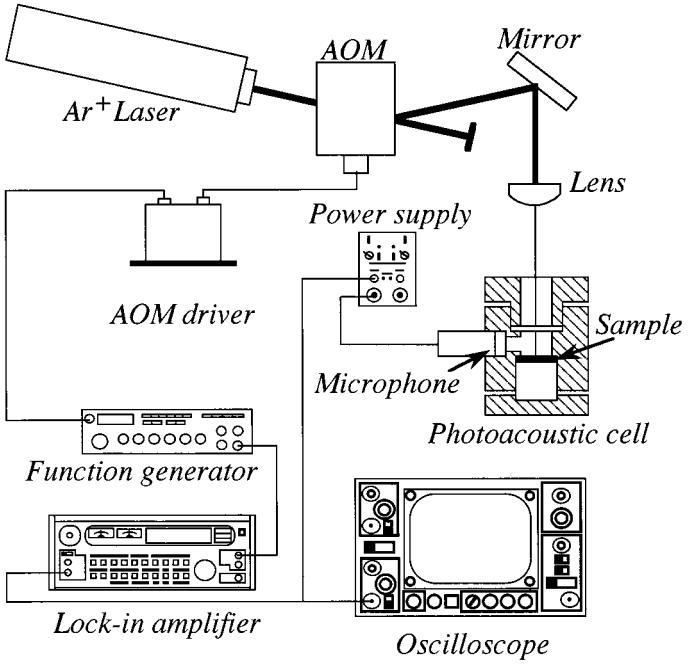

Fig. 3. Schematic diagram of experimental apparatus.

used as a light source. The continuous beam from the source is transformed into an intermittent beam of the first-order diffraction by an acoustooptic modulator (AOM). The frequency of the intermittent beam can be controlled by a function generator. After the beam is condensed by a lens, it passes through a window made from BK7-glass of a photoacoustic cell, and then is intermittently irradiated and absorbed at the sample. The acoustic wave is induced in the cell and reaches a microphone with a preamplifier. The frequency range is from 2.6 to 10 kHz. The output signal is introduced to a lock-in amplifier with the signal from the function generator and is checked by an oscilloscope. Then the phase lags between these signals and the amplitude of the output signal are determined. In the present study, the phase lag data are used to determine the thermal diffusivity of the sample because of its high sensitivity compared with the amplitude. The measured precision of the phase lag is better than 0.1 deg.

Figure 4 shows the details of the photoacoustic cell. It is made of transparent acrylic resins because if the reflected light on the sample is absorbed at the side walls, the acoustic wave is newly induced and is mixed with that induced from the sample. The air space in the cell is sealed by the

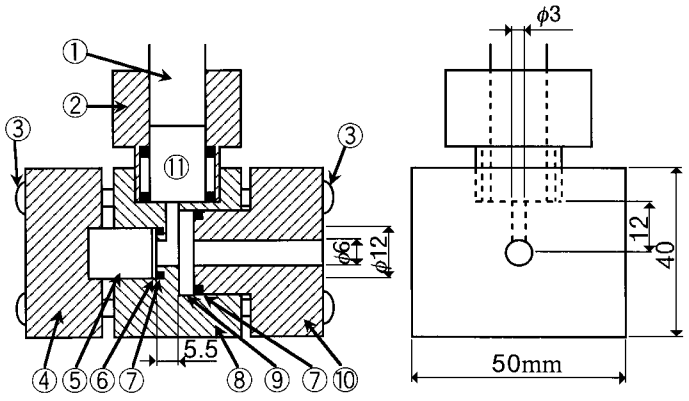

Fig. 4. Details of photoacoustic cell.

window and the sample with the backing by using screws. The total volume is 220 mm^3 with a distance of 5.5 mm between the window and the sample and a column diameter of 6 mm, considering the signal amplitude, a one-dimensional treatment of the phenomena, and visual observation of the incident condition. The cell is arranged so that the microphone does not receive the reflected light.

The measured data on the phase lag in the actual state are different from the theoretically predicted values in the idealized state because of several factors peculiar to the present apparatus, such as the shape of the air space in the photoacoustic cell. In order to eliminate the difference, the measurements for the calibration are carried out by using a thick sample. As the thickness increases, the region of the constant phase lag at the right side of Fig. 2 expands in the present modulation frequency. According to the RG theory, it is assumed that the phase lag under the optically and thermally thick condition is 45 deg regardless of the modulation frequency and the material. Therefore, the phase lag shown in Eq. (1) is calculated by the equation

$$\varphi = \varphi_{\mathrm{mea}} - (\varphi_{\mathrm{ref}} - 45) \tag{2}$$

where φ_{mea} and φ_{ref} are the actual data of the unknown sample and the reference sample for the calibration, respectively. The reference samples are

titanium and nickel plates having thicknesses of 14.0 and 15.6 mm, respectively. Both data sets agree well and must be kept constant at 45 deg.

4. RESULTS AND DISCUSSION

Figure 5 shows the experimental data on the phase lag of the photoacoustic signal versus the modulation frequency of incident irradiation for titanium foils. These foils are made by rolling and have a stated purity of 99.5%. They are mounted on a backing made of transparent acrylic resins by epoxy resin glue. The solid curves shown in Fig. 5 indicate the fit of the experimental data by the RG theory. The fitted curves agree well with the experimental data. The thermal diffusivities of the samples are obtained within a precision of 5%. The difference in thickness of the titanium foils causes a shift of the peak frequency of the phase lag, as is explained by the RG theory. Figure 6 shows the experimental data and the fitted curves of the phase lag for sputtered thin films produced on the glass substrate. The deposition rates of titanium and nickel are 52 and 102 $nm \cdot min^{-1}$ in argon atmosphere at 6.7×10^{-1} and 6.0×10^{-1} Pa, respectively. The fitted curves agree well with the experimental data over the complete frequency region including the peak in the same manner as in Fig. 5. There is a difference in the peak frequency and the peak value of the phase lag between titanium and nickel because of differences in thermophysical properties.

Figures 7–10 show microphotographs of titanium foil, stainless steel (SUS304) foil, titanium-sputtered film, and nickel-sputtered film, respectively. The foils shown in Figs. 7 and 8 are considered to be a continuous

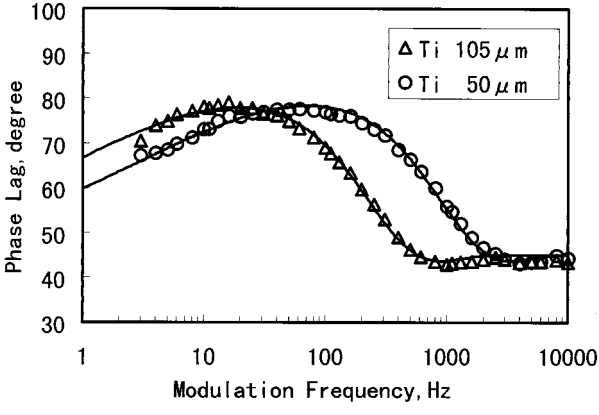

Fig. 5. Experimental data and fitted curves of phase lag vs. modulation frequency for titanium foils.

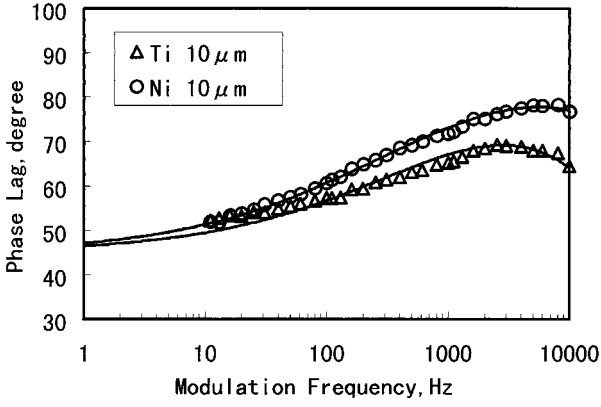

Fig. 6. Experimental data and fitted curves of phase lag vs. modulation frequency for titanium and nickel sputtered films.

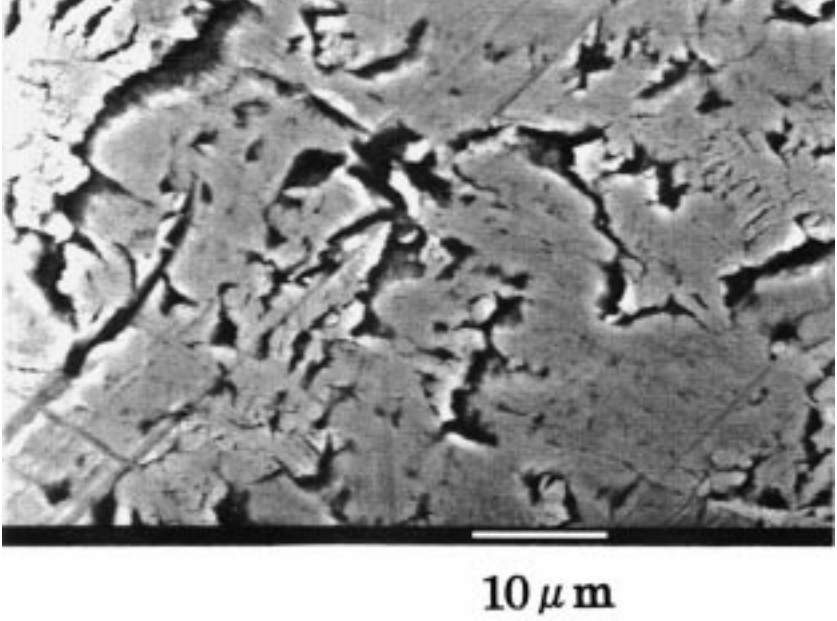

Fig. 7. Microphotograph of titanium foil of 50 μm thickness ($\times$2000).

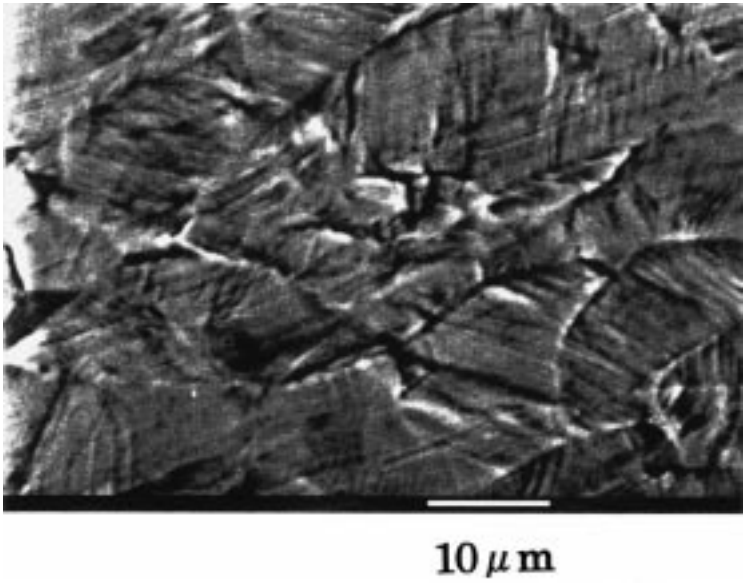

Fig. 8. Microphotograph of SUS304 foil of 50 μm thickness ($\times$2000).

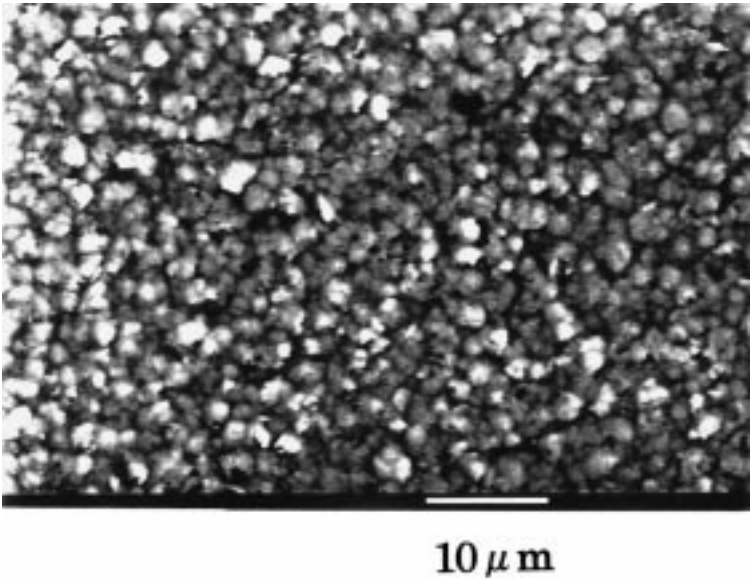

Fig. 9. Microphotograph of titanium sputtered film of 10 μm thickness ($\times$2000).

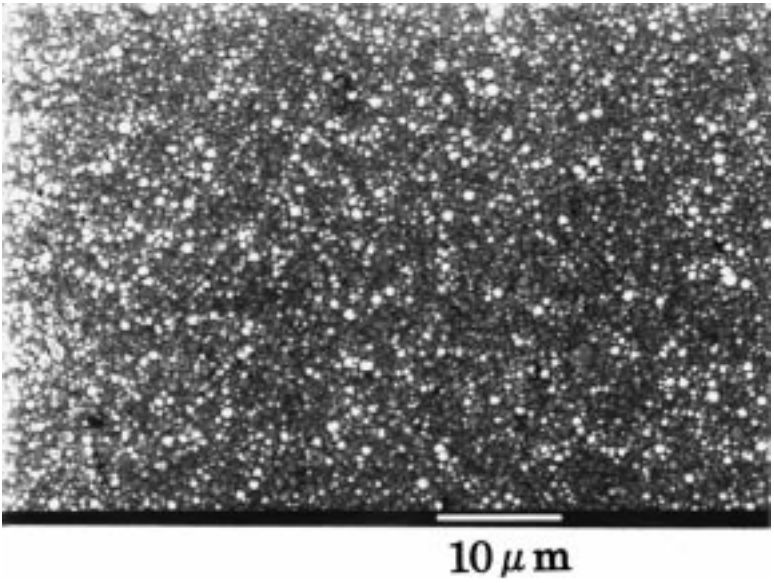

Fig. 10. Microphotograph of nickel sputtered film of 10 μm thickness ($\times$2000).

body, but some gaps are recognized in Fig. 7. The sputtered films shown in Figs. 9 and 10 are composed of fine particles which are piled up and fused. The typical particle size of nickel is smaller than that of titanium, and the structure of nickel film is denser than that of titanium film.

Figure 11 shows the thermal diffusivity of titanium foils and sputtered films as a function of the thickness. The present results have a reproducibility within 5%. The thermal diffusivity of the foils of 105 and 160 μm thickness agrees with the published value of the plate [5], but is larger than that of the 10-μm-thick sputtered film because of the differences in the fine structure. In the cases of foils with thicknesses of 20 and 50 μm, the thermal diffusivities are smaller than published values [5] because the gaps in the foils, as shown in Fig. 7, may affect the heat conduction. The data of Akabori et al. [2] obtained by the same method are also shown in Fig. 11, and are smaller than the present data. Some of the causes may well be the fine structure of the sample and the backing material.

Figure 12 shows the thermal diffusivity of SUS304 foils as a function of thickness. The present results have a reproducibility within 4% to 5%. Compared with titanium, the thermal diffusivity is independent of the thickness, although a scatter of the results can be seen to some degree. The thermal diffusivity of the foils agrees with the published value of the plate [5].

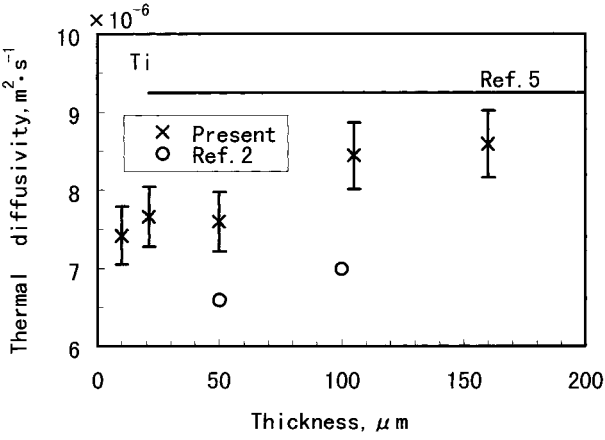

Fig. 11. Experimental results for the thermal diffusivity of titanium foils and sputtered films vs. thickness.

Table I summarizes the present data on the thermal diffusivity of titanium, nickel, stainless steel (SUS304), and platinum. The nickel and platinum foils have a stated purity of 99.69 % and 99.98 %, respectively. The present data for the foils agree well with the published value [5] except for the thin foils of 20 and 50 μm thickness for titanium and of 50 μm thickness for SUS304. As for the sputtered film of nickel, the thermal diffusivity is almost the same as that of the foil, which exhibits different behavior from titanium because of the fine structure, as shown in Figs. 9 and 10.

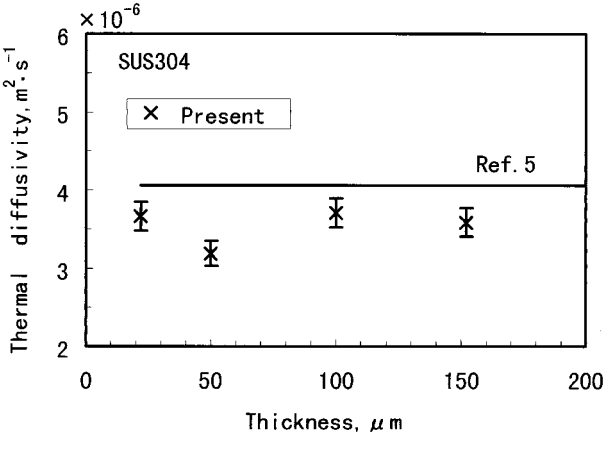

Fig. 12. Experimental results for the thermal diffusivity of SUS304 foils vs. thickness.

Table I. Experimental Results for the Thermal Diffusivity of Metallic Foils and Sputtered Films

Material	Thickness (μm)	Thermal diffusivity ($10^{-6}\,m^2 \cdot s^{-1}$)	
		Experiment	Ref. 5
Titanium	160	8.59	9.25
	105	8.44	
	50	7.60	
	21	7.66	
	10	7.42	—
Nickel	200	20.7	22.9
	10	22.1	—
SUS304	152	3.59	4.07
	100	3.71	
	50	3.19	
	22	3.67	
Platinum	105	22.9	25.2

If the thermophysical properties of the backing are given, the thermal conductivity of the sample can be determined as described earlier. In the present study, the backing materials are acrylic resins for the foils and glass for the sputtered films. We assume that the thermal conductivity and the thermal diffusivity of the backing are $0.21\,W \cdot m^{-1} \cdot K^{-1}$ and $0.12 \times 10^{-6}\,m^2 \cdot s^{-1}$ for acrylic resins, and $1.10\,W \cdot m^{-1} \cdot K^{-1}$ and $0.68 \times 10^{-6}\,m^2 \cdot s^1$ for glass, respectively [5]. The results for the thermal conductivity of titanium with thicknesses of 160, 105, 50, 21, and 10 μm are 18.7, 19.5, 19.2, 17.6, and $16.3\,W \cdot m^{-1} \cdot K^{-1}$, respectively. These values are in reasonable agreement with the published value of $21.9\,W \cdot m^{-1} \cdot K^{-1}$ [5] in spite of the estimated thermophysical properties of the backing.

5. CONCLUSIONS

The thermal diffusivities of metallic thin foils of several thicknesses were obtained by analysis of the measured spectral data of the induced phase lag of sound by the cyclic irradiation on the sample in a closed cell based on the RG theory. The measured results agreed with literature values except for the thin foils with microscopic gaps. The thermal diffusivities of thin films produced by sputtering were also measured in the high-frequency region and the measured results compared with those of foils. It was clear that the microscopic structure of the samples affected the results.

ACKNOWLEDGMENTS

The authors wish to thank K. Yamanishi of Mitsubishi Electric Co. for providing the samples and Prof. Y. Nagasaka of Keio University for his valuable information. Thanks are also extended to a former student, T. Shimizu of Okayama University, for his contribution in the initial stage of the present study.

REFERENCES

1. A. Rosencwaig and A. Gersho, *J. Appl. Phys.* **47**:64 (1976).
2. M. Akabori, Y. Nagasaka, and A. Nagashima, *Int. J. Thermophys.* **13**:499 (1992).
3. F. A. Mcdonald, *Appl. Phys. Lett.* **36**:123 (1980).
4. T. R. McCalla, *Introduction to Numerical Methods and FORTRAN Programming*, 1st Ed. (Wiley, New York, 1967).
5. K. Kobayashi, ed., *Thermophysical Properties Handbook*, 1st Ed. (Yokendo, Tokyo, 1990).